Low-cost Chirp Linearization for
Long Range ISAL Imaging Application

Hanying Zhou[*], Bijian Nemati, Mike Shao, Chengxing Zhai
Inseob Hahn, William Schulze, Russell Trahan
Jet Propulsion Laboratory, California Institute of Technology, Pasadena, CA 91109, USA

ABSTRACT

High quality linear laser frequency chirp of high chirp rate is critical to many laser ranging applications. In this paper, we describe a cost-effective chirp linearization approach implemented on our Inverse synthetic Aperture LADAR (ISAL) imaging testbed. Our approach uses a COTS PZT for external cavity laser frequency tuning and a common self-heterodyne fiber interferometer as a frequency monitor, with a two-step hardware and software chirp linearization procedure to achieve high quality chirp. First, the nominal triangle waveform input to PZT drive is modified through an iterative process prior to ISAL imaging acquisition. Several waveforms with chirp rates between 1 and 4THz/s have been acquired with residual chirp rate error ~ +/-2% in usable region. This process generally needs to be done only once for a typical PZT that has excellent repeatability but poor linearity. The modified waveform is then used during ISAL imaging acquisition without active control while the imperfection in transmitted frequency is monitored. The received imaging data is resampled digitally based on frequency error calculated from the frequency monitor data, effectively reduce chirp nonlinearity to ~+/-0.2% in chirp rate error. The measured system impulse response from return signal shows near designed range resolution of a few mm, demonstrating the effectiveness of this approach.

Keywords: Chirp linearization, inverse synthetic aperture LADAR (ISAL), long-range imaging, PZT waveform modification, chirp resampling, air turbulence phase piston on chirp length, chirp impulse response, frequency monitor

1. INTRODUCTION

Inverse synthetic aperture radar (ISAR) has been successfully used in imaging asteroids for decades [1]. In recent years its optical counterpart, inverse synthetic aperture LADAR (ISAL), is being explored for potential higher sensitivity and higher resolution imaging of asteroids or other near-earth objects such as GEO space objects [2, 3]. ISAL shares many similar principles as regular synthetic aperture LADAR (SAL) [4 -6], except it relies on target's rotation to form 2D image. Like many other laser ranging applications, ISAL uses linear frequency modulation (LFM) to increase signal's bandwidth. Since nonlinearity in the chirp degrades the resolution and causes ambiguity in range if not mitigated, the ability to generate high quality linear laser frequency chirp of wide bandwidth (~THz) with sufficient coherence become critical to these applications. For ground-based long range imaging application where chirp length can be constrained by air turbulence effect, high chirp rate in ~multi THz/s is more important (in achieving needed bandwidth).

One frequently used technique to linearize laser chirp frequency is through active feedback control with a self-heterodyne fiber delay interferometer. A phase detector, such as a digital phase detector or an EO phase [7, 8] can be used to detect the error between the transmitted signal and a reference (electronic) signal and then fed back to laser to phase lock laser. This method can achieve high precision laser frequency control: frequency error better than 0.2MHz for a ~ 5THz bandwidth has been reported with a resolution of ~30μm [8]. The downside of this approach is its cost and complexity in modulation hardware, when μm resolution is unnecessary for imaging objects tens of thousands km away (cm or mm at most is sufficient).

Other linearization techniques that have been successfully used for applications at much lower chirp rates (~tens of GHz/s) or bandwidth include resampling the interference signal to correct the nonlinearity and frequency modulation waveform pre-distortion. For example, in optical frequency domain reflectometer system for diagnosing optical fibers, a common

_____

*hanying.zhou@jpl.nasa.gov

method is to use an auxiliary interferometer to monitor the laser frequency, and then use this information to resample the interference signal to correct the nonlinearity in frequency chirp [9]. Recently a frequency modulation waveform modifying technique, also works at low chirp rates of tens of GHz/s, is reported [10]. It uses an Analog Digital Converter to FFT analyze the beat frequency waveform captured by an oscilloscope and then reconstructs a new FM waveform with a commercial Waveform Builder software. This reduces the chirp nonlinearity, but by itself, is far from enough for the needed frequency accuracy for the chirp rate required.

In this paper, we report a cost effective chirp linearization method for THz/s chirp rates used in our ISAL imaging testbed. Our approach uses a PZT for external cavity frequency tuning and a self-heterodyne interferometer to obtain chirp rate error information. Chirp nonlinearity is compensated in two stages: a coarse hardware correction *a prior* to the imaging acquisition (through PZT control waveform modification), and then a more accurate software correction (resampling) with the imaging data. In the following details of the method is described after a brief description of our testbed and its main components for chirp generation.

2.   ISAL TESTBED AND CHIRP GENERATION

Our testbed, shown in Fig.1, consists of a solid state tunable laser, a frequency monitor, a transmitter and a receiver, and a data acquisition system (not shown). Two pairs of AOMs are used for shifting DC to desired carrier frequency. The bistatic configuration is chosen for the simplicity of a low budget testbed.
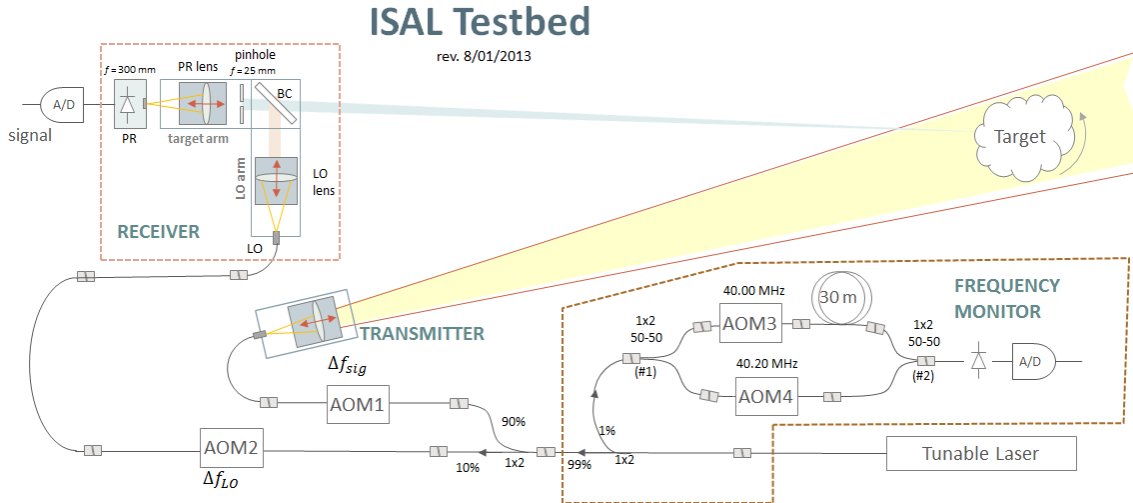
Figure 1: Inverse Synthetic Aperture Lidar (ISAL) testbed layout.

The laser generates a liner chirp near 1.3um with output power ~50mW. A small fraction (1%) of the light is diverted to a frequency monitor consisting of a self-heterodyne fiber interferometer. The remainder of the light is split again, to the transmitter (90%) and the local oscillator (10%). The transmitter assembly launches this light towards a rotating target. The light reflects off of a target and is collected by the receiver. At the receiver, the return from the target is mixed with the local oscillator, a delayed, frequency-shifted version of the transmitted light, producing a heterodyne signal that can be detected by a photo-sensitive device. Heterodyne mixing of the light brings the signal down to the bandwidth accessible to electronic devices and amplifies the signal-to-noise ratio as well. The target range information can then be found from the beat frequency of the de-chirped receiver data.

We used Thorlabs TLK-1300R Littrow external cavity tunable laser. It comes with a standard servo motor to move the grating to adjust the laser frequency, with a 10 dB tuning range of 130 nm for center wavelength of 1310 nm and coherence length ~3km. However, the standard servo is unable to move fast enough to provide chirps on the order of THz/s needed for our application, we therefor replaced it with a COST PZT actuator, also from Thorlab, DRV181. This PZT has a maximum travel distance of about 80nm and is able to provide a tuning range of about 22 nm at rates up to about 4 THz/s.

It is powered by its controller which takes an arbitrary waveform as its input. The whole laser and PZT assemble is shown in Fig. 2a.

The frequency monitor used to measure the chirp rate shares the same heterodyne detection principle as the main transmitter – target – receiver system, except that the range is known and fixed with a delay fiber. As shown in Fig..1, the interferometer splits the laser light, produces a delay in one arm and then remixes the two arms. The result is a waveform whose frequency is the change in the frequency or chirp rate. Since the delay is fixed and signal is strong (no noise), the mixed signal is generally a pure sinusoid signal whose frequency is proportion to the chirp rate being monitored. This knowledge of transmitted chirp rate (and thus its error from the ideal one) provides the basis for both hardware and software chirp linearization described in Sect. 3 and 4.
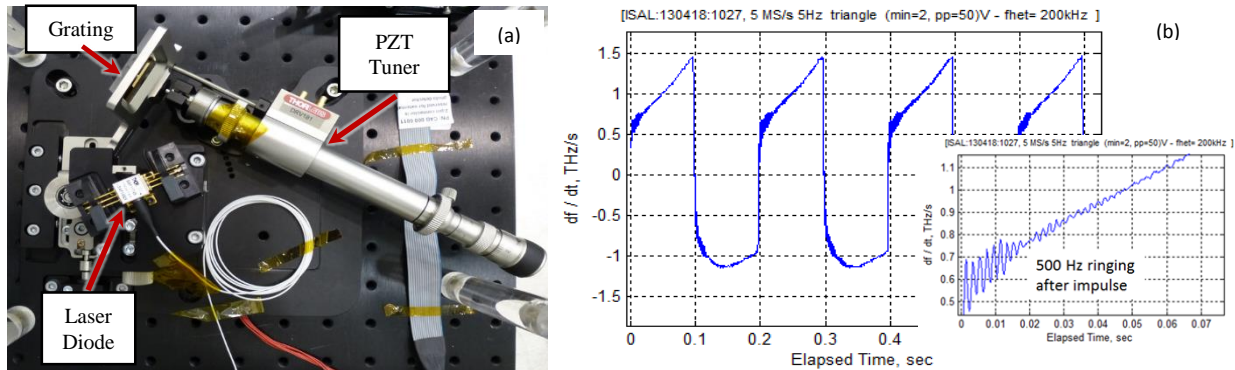
Figure 2 a). Thorlabs TLK-1300R Littrow tunable laser with the modified PZT tuner. b) Measured chirp rate profile with PZT driven by a triangle waveform. Insert: close-up of the ringing at the beginning of up ramp

To generate a linear chirp, nominally a waveform of the same frequency pattern is applied to PZT to tune the laser frequency, e.g., a triangle waveform to generate triangle frequency pattern (= linear chirp). In reality, the mechanical operation of PZT is imperfect, so the chirp produced is rather nonlinear if directly driven by a triangle waveform. Fig. 2b shows a typical measured chirp rate profile from the frequency monitor. While the average chirp rate is at the designed level, there is large nonlinearity in both up and down ramps (a perfect linear chirp would have flat or square wave chirp rate). Additionally, there is ringing in the chirp rate profile seen (the insert) after each PZT direction reversal reflecting mechanical strain in the grating assembly at turnarounds, as the PZT has a finite frequency response.

3. HARDWARE CHIRP LINEARIZATION

3.1 PZT waveform modification

Obviously the nominal chirp as generated by a triangle waveform input to PZT need to be improved. Our first step is through hardware linearization. As can be seen partially in Fig. 2b, despite the large nonlinearity, the chirp rate pattern is quite repeatable over a couple of hundred chirps that we typically use for imaging purpose. This repeatability makes it feasible to improve chirp nonlinearity in hardware by applying a modified waveform to PZT drive that pre-compensates the chirp nonlinearity. Additionally we opt to linearize just portion of chirp, i.e., we ignore a small turnaround portion of chirp to ease the hardware chirp linearization. This would mean to use only portion of data from each chirp during imaging reconstruction which can be done fairly easy in software. The whole process is done through an iterative process prior to ISAL imaging acquisition as follows.

We start with a triangle wave with rounded corners; the rounding is to reduce the ringing at the PZT turnaround and is achieved by using a moving window averaging filter to smooth the triangle waveform. This corner-rounded initial "perfect" triangle control waveform is then fed to the wave generator of PZT controller. Next take a short test data and find chirp frequency and chirp rate from frequency monitor data. This is accomplished by binning the monitor time series voltage data in small batch, find its mean frequency (change) by taking FFT (zero padded for better frequency resolution) and

locating the peak, and then converting the result into chirp rate (and integrate the chirp rate to get chirp frequency). Take one cycle of measured chirp and then compare it to the "perfect" wave to determine the error. Here care must be taken since there are time delays incurred in the data path through the waveform generator, the PZT controller, the PZT, the optical system, the photoreceiver, and the DAQ, the measured frequency response must be time-shifted before computing the error between the control waveform and response waveform correctly. Once the error is computed, the PZT control waveform is adjusted by adding the error waveform subject to a loop gain (typically ~0.5). Often the amount of the time shift often is not precisely known initially, and so is subject to adjustment in each iteration as well. The process, as illustrated in Fig.3, is repeated for a few times:

$$wf_n(t) = wf_{n-1}(t) + G \cdot \left[rsp_{n-1}(t - \tau_{n-1}) - wf_p(t) \right] \qquad (1)$$

where $wf_n(t)$ is the PZT waveform after nth iteration, $rsp_{n-1}(t - \tau_{n-1})$ is the frequency response at $(n-1)$th iteration shifted by amount of τ_{n-1}, G is loop gain, and initial waveform is set to be the perfect waveform: $wf_o(t) = wf_p(t)$.
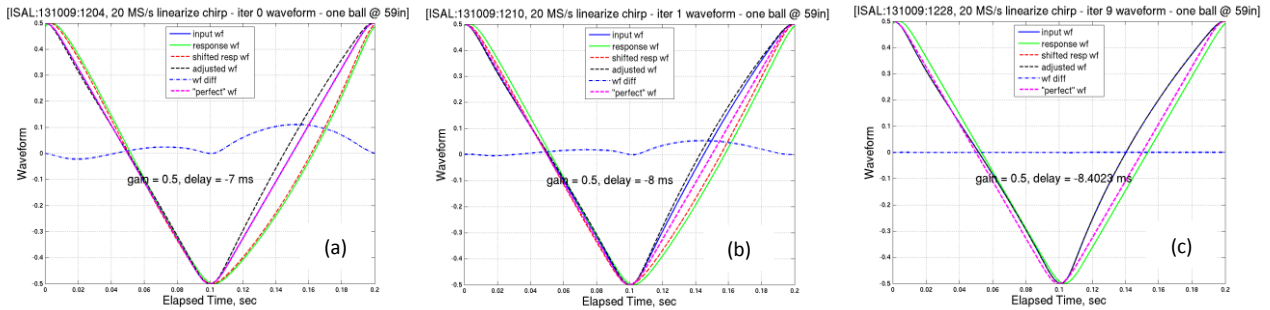
Figure 3: Iteratively adjusting waveform based on measured frequency error: a) At initial iteration, the input PZT control waveform (blue line) overlaps with the ideal waveform (dash magenta), while the (raw) frequency response (green line) has a large difference from the ideal one. The frequency response wave is time shifted (dash red) before being compared to the ideal one for correction amount calculation. Dot-and- dash blue line indicates peak error in frequency >10%. b). After one iteration, the modified control waveform (blue line) now departs from the ideal waveform (dash magenta) while the time-shifted frequency response is bit more close to the ideal waveform. c).At iteration #9, the time shifted frequency response essentially overlaps with ideal waveform (dash red and dash magenta), indicating a much diminished frequency error

Figure 4 shows the resulting chirp frequency and chirp rate from the nonlinearity pre-compensated waveform of Fig. 3b. Clearly, the chirp rate during each ramp is now essentially constant except for effect of vibrations at a small level. Compared to Fig.2a, improvement in chirp rate is significant, with residual chirp rate error better than +/-2%, about ~25x improvement compared with the raw chirp rate, and much smaller in chirp frequency after integration. Since the PZT has excellent repeatability, the above iterative process to generate chirp nonlinearity pre-compensated waveform generally needs to be done only once for a given chirp rate prior to ISAL imaging acquisition.
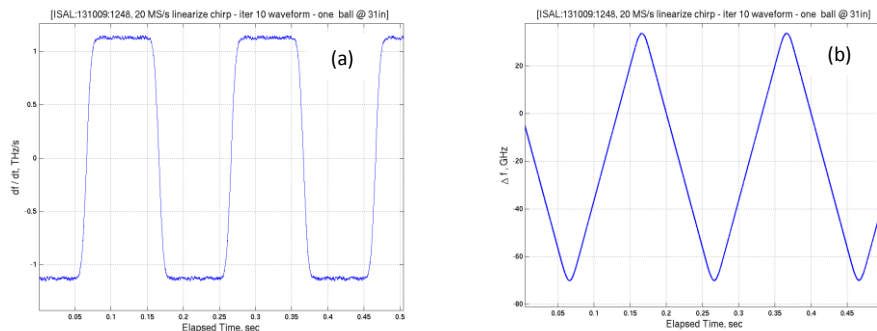
Figure 4: Chirp rate (a) and chirp frequency (b) profiles, as measured by the frequency monitor after hardware linearization. The chirp rate error residual better than +/-2%.

3.2 Chirp Duration and Chirp Rate as Affected by Air Turbulence Piston Effect

Our nominal design range resolution is slightly less than 2mm with a 1THz/s chirp rate and 100ms chirp duration combination (~80% actual chirp duration used and broadening effect with FFT windowing for sidelobe suppression). Above 1THz/s control waveform is more than sufficient (with further software linearization, details in Section 4) to achieve the expected resolution during our prototype laboratory demo at a relatively close range distance (a few meters). For outdoor ISAL imaging demo, chirp duration must be shortened. This is because for most ground-based long range imaging applications, the atmospheric effect would put a limit on maximum chirp length allowed within which the phase errors in received signal can be effectively corrected with range Doppler compression algorithms. In fact, the air turbulence and available laser power place conflicting constraints on desired chirp length: short chirp length preferred to minimize air turbulence effect on range ambiguity, but long chirp length desired to maximize the return photon not too lower than one photon per range bin. It is important to strike a balance between two.

While air turbulence impact on ISAL imaging is complicated and needs more study [11], as a first order, the macro-scale turbulence piston effect can be measured and used to guide the selection of appropriate chirp length. We used the same ISAL testbed setup but with non-chirped signal to measure atmospheric piston error. When a non-chirped signal is transmitted, the received signal should be of a constant (carrier) frequency (set by AOM) with constant phase if no air turbulences present. Any phase fluctuations in the return signal at the carrier frequency then indicates the roundtrip optical path change by air turbulence. To remove any instability by transmitter itself we subtracted out the phase of monitor carrier frequency. In another words, the air piston error is calculated as the difference between two carrier frequency's phases.

Two metrics are currently used to determine the appropriate chirp length for a given atmosphere condition. First, for consecutive pulse-to-pulse phase error (which affects cross range phase connection and its compression quality), the Allan deviation of the air piston phase, $\sigma_A(\tau)$, is used to assess the air phase stability. Allan deviation can be expressed as the standard deviation among the differences between consecutive segment's mean:

$$\sigma_A(\tau) = \sqrt{\frac{1}{2}\langle(\bar{\phi}_{n+1} - \bar{\phi}_n)^2\rangle} \qquad (2)$$

where $\bar{\phi}_n$ is the mean air phase of nth segment data of length τ. For intra-chirp phase error (which causes return signal's range spread or displaces return signal into nearby range bin or even splits return signal from a single scatterer into multiple range bins), we first consider the standard deviations of air phases in each segment, $\sigma_n(\tau)$:

$$\sigma_n(\tau) = \sqrt{\langle(\phi_n - \bar{\phi}_n)^2\rangle}, \qquad (3)$$

and then use the statistics of these standard deviations, $\sigma_p(\tau)$:

$$\sigma_p(\tau) = (\text{up to}) \ \bar{\sigma}(\tau) + z * \sqrt{\langle(\sigma_n(\tau) - \overline{\sigma_n(\tau)})^2\rangle} \quad (4)$$

to determine maxima allowable air phase piston with one-sided upper confidence level z =0,1,or 2 (corresponding to 50%, 84%, or 98% confidence levels, respectively).

Figure 5 shows one example of a 50m round trip air piston measurement and its statistics. Use threshold phase piston error <1 rad RMS for both inter-chirp and intra-chirp (at confidence level of 98%), we can see the chirp duration needs to be ~10ms or shorter for this particular air turbulence condition, and is mostly restricted by intra-chirp phase error (for inter-chirp, both <10ms or >65ms would satisfy <1 rad criteria). Simulation of this measured air piston phase error added to an ideal signal with chirp length choice of 10, 20, and 30ms confirms that a chirp length of ~10ms would limit chirp width broadening within acceptable range (~1.1 times), while chirp length of ~20ms would causes broadening by1.5x and 30ms by 2x, too large.

In several repeated measurements, acceptable chirp duration was found to vary between ~4ms (worst, midafternoon) to ~50ms (benign, late evening) depending on time and date when a test was taken (the test itself was conducted on rooftop). We then choose to have imaging acquisition done at relatively "good" realistic air turbulence conditions. This would mean

to use chirp length 20~40ms mostly (which is roughly in line with typical vertical atmosphere coherence time of 15~40ms for wavelength 1~2um, for ground-based space object imaging application).
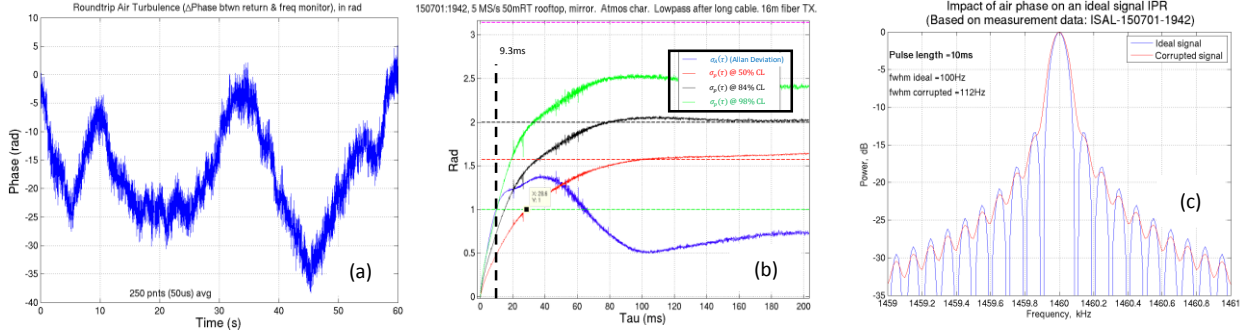
Figure 5: a) Example of a round-trip air phase piston measured. b) Deviations in air phase fluctuation c) Simulation with measured air phase error of a) shows acceptable chirp width widening after limiting chirp length

Since range resolution inversely proportion to both chirp rate β and chirp duration T: $\delta R = c/2\beta T$, to maintain adequate range resolution, higher chirp rates are needed. Using the same procedure as in Section 3.1, we generated waveform for 2 ~ 4Thz/s chirp rates as shown in Fig.6, for use with shorter chirp duration. Slightly increased ringing can be seen again at one turnaround direction (down ramp), reflecting a more demanding PZT response need for higher speeds. This is currently not of a big concern for our ISAL imaging purpose: as up and down ramps chirp data are processed separately, each forms independent image on the two sides of carrier frequency and only one is needed
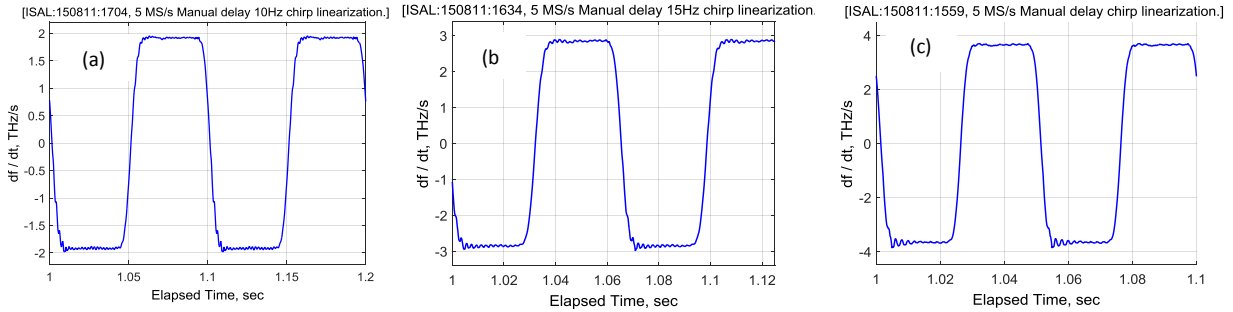
Figure 6: PZT control waveforms for chirp rates 2 ~ 4THz/s, with residual chirp rate nonlinearity ~+/-2% in usable region of up ramps.

4. SOFTWARE CHIRP LINEARIZATION

4.1 Chirp Resampling

The improved PZT control waveform as above can be used during ISAL imaging acquisition without active PZT control while the residual imperfection in transmitted frequency is monitored. As mentioned above, the modified PZT actuation waveform greatly improved chirp quality, but the residual nonlinearity still exists: ~2% or +/-2GHz/s for 1THz/s chirp rate. To further minimize the nonlinearity, our second step is to use frequency monitor data to resample the receiver imaging data to remove the nonlinearity in chirp. In theory, if imaging data is Nyquist sampled, it can be resampled to remove imperfectness in chirp without added noise. We typically use 5Ms/s to 20Ms/s data sample rates for imaging acquisition depending on the chirp rates used.

The idea here is that the deviations in the chirp from ideal LFM are captured by the frequency monitor and timestamped at equal increments in time. Manipulating these timestamps is akin to changing the frequency of the return signal thus distorting time in the data can emulate changing the frequency of the laser. The task is therefore to create a pseudo timestamps in which the chirp is perfectly linear and IPR is optimized.

Recall that the de-chirped signal from the frequency monitor is a pure sinusoid, whose frequency is determined by the (fixed) fiber delay and instant chirp rate, offset by the carrier frequency set by the AOMs:

$$S(t) = A \, \cos\left[2\pi\left(\Delta f_{AOM} + \beta \, \delta t\right)t + 2\pi \int_0^t \delta f(\tau) \, d\tau\right], \qquad (5)$$

$$\delta f \equiv \left(\frac{df}{dt} - \beta\right) \delta t \qquad (6)$$

here we separate instant chirp rate, df/dt, into its ideal component β (constant throughout all chirps) and the deviation part, $\delta f/\delta t$, δt is the fixed fiber delay.

The pseudo time t' is then defined to make the chirp purely linear:

$$S(t') = A \, \cos\left[2\pi\left(\Delta f_{AOM} + \beta \, \delta t\right) t'\right] \qquad (7)$$

Setting the two expressions for S equal yields:

$$t' = t + \frac{\int_0^t \delta f(\tau) \, d\tau}{\Delta f_{AOM} + \beta \, \delta t} \qquad (8)$$

Or in discrete form:

$$t'_n = t_n + \left[\frac{\tau_s \cdot \delta t \cdot \sum_{i=1}^n \left(\frac{df}{dt}\right)_i}{\Delta f_{AOM} + \beta \, \delta t}\right], \qquad (9)$$

where τ_s is data sampling interval.

Note that the pseudo time depends on the delay δt as well as carrier frequency. Replace fixed fiber delay δt with mean target delay, and frequency offset Δf_{AOM} of monitor AOM with that of receiver AOM, above equations apply to receiver data resampling as well.

The procedure for resampling can then be described as follows: First we find chirp frequency and chirp rate from frequency monitor data, as we have done during hardware chirp linearization described in Sect 3.1. Currently the binning of batch data to find frequency uses non-overlapping data points (for processing speed), the result chirp data need to be interpolated to fill in the interior points of time (so it has matching time stamps as the receiver data again). Next for each chirp, we find the frequency error and pseudo time stamp for nth sample in the usable chirp portion as Eq. (9). Finally we interpolate the original imaging data, chirp by chirp, (back) to the regular time spacing t, as if the original receiver data was sampled at the irregular time spacing t'.

Figure 7a shows a comparison of the chirp rate before and after the post-processing linearization for 1THz/s chirp rate. Clearly, prior to the post processing the chirp rate has small ripples in each up and down chirps. After resampling the chirp rate is effectively maintained to 1.14 THz/s ±0.002THz/s (or better than +/- 0.2%) in the region used for subsequent imaging /autofocusing. In terms of chirp frequency, the standard deviation of nonlinearity is within ~1.5MHz, more than sufficient for intended mm range resolution application.

It is worth noting that the residual frequency error in the final software-linearized chirp is currently limited by the frequency resolution during FFT analyzing monitor data for chirp frequency and rate. Since we typically use non-overlapping data batch (to reduce the number of FFTs needed), the neighboring frequency values have time interval of the batch size (we then interpolate to get the frequency values at the interior points between two adjacent time indices), which reduces the FFT interpolation based frequency resolution. For a typical 1000 data points binning, 5MS/s sampling rate and 8x zero padding for FFT interpolation, the frequency resolution is just under 1MHz. While this has no noticeable effect on the final

imaging quality (as the resolution is already adequate), it is possible to further reduce chirp nonlinearity error through either increasing data sampling rate, increasing zero padding in FFT finding frequency, or using overlapped data points in
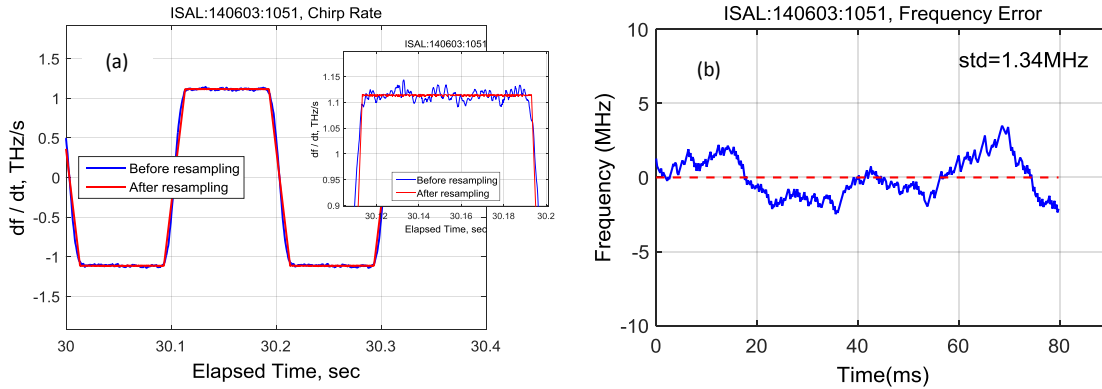
Figure 7: a) Chirp rates before (blue) and after (red) resampling; chirp rate error is within +/-0.2%. b) After integration and linear portion subtracted, the chirp frequency error shows having a standard deviation < ~1.5MHz.

4.2 Chirp Quality as measured by IPR

While linearity in frequency is a good indication of a quality linear chirp, a better chirp quality measurement would be Impulse Response (IPR), which has been widely used in the field of SAR. It characterizes chirp behavior that passes reflected response or incidental periodic modulation (e.g., amplitude modulation). IPR is basically a system's response to a point object; as such, it can be readily measured using a small specular ball with the testbed. For a specular curvy surface such as polished metal ball, the light power reflected back to the receiver is nearly zero from all but a very small region (~tens of nm with a 1" size metal ball for our setup) with angle normal to the surface, effectively making it a point object.

In one of the test data taken, we used three 1" shiny balls for simple 2D ISAL imaging demo. FFT the de-chirped return signal chirp by chirp, and then average over ~200 chirps, the IPR, which is the resulting normalized PSD from largest ball return in log scale, is shown in Fig 8. The estimated FWHM at -3dB of measured IPR is 11.5 Hz, close to the ideal time window limited FWHM of 11.2Hz (all without windowing during FFT for this purpose). In terms of image resolution, this will have a mere 0.04mm increase, well within the design tolerance. The shape of IPR is quite symmetrical, indicating no significant system error. The quality of chirp is also demonstrated through our successful ISAL imaging reconstruction with under low CNR (~<0.4) and in presence of atmosphere turbulence as detailed in another paper [2].
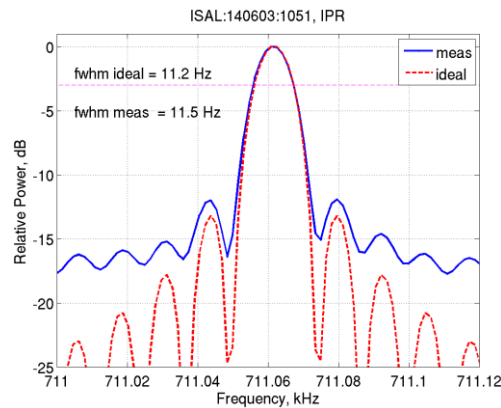
Figure 8: Measured (blue) and ideal (red) IPRs of transmitted chirp

5. SUMMARY

We have demonstrated a very cost-effective chirp linearize approach for our ISAL imaging testbed with a PZT for external cavity laser frequency tuning and a self-heterodyne fiber interferometer as frequency monitor. The PZT waveform modification improves raw chirp nonlinearity by ~25x to about +/-2% residual chirp rate error. The software resampling further improves another ~10x to about +/- 0.2% in residual chirp rate error for chirp rates 1~4 THz/s, or <2MHz in chirp frequency error for 1THz/s chirp rate. The measured system IPR from return signal shows near designed range resolution of a few mm, demonstrating the effectiveness of this approach.

6. ACKNOWLEDGMENTS

REFERENCES

[1] Ostro, S. J., Hudson, R. S., M. Benner, L. A., Giorgini, J. D., Magri, C., Margot, J. L., and Nolan, M. C., "Asteroid Radar Astronomy," in [Asteroids III], Bottke, W. F. Jr., Cellino, A., Paolicchi, P., and Binzel, R. P. (eds), Univ. of Arizona Press, Tucson, 151-168 (2002).

[2] Trahan, R., Nemati, B., Zhou, H., Shao, M., Hahn, I., Schulze, W., "Low-CNR Inverse Synthetic Aperture LADAR Imaging Demonstration with Atmospheric Turbulence," Proc. SPIE. 9846, (this conference) (2016)

[3] Pellizzari, C. J., Matson, C. L., Gudimetla, V. S., "Inverse synthetic aperture LADAR for geosynchronous space objects—signal to noise analysis," Proceedings of the 2011 Advanced Maui Optical and Space Surveillance Technologies Conference (AMOS), (2011).

[4] Bashkansky, M., Lucke, R. L., Funk, E., Rickard, L. J., and Reintjes, J., "Two-dimensional synthetic aperture imaging in the optical domain," Opt. Lett., 27 (22), 1983-1986 (2002)

[5] Beck, S. M., Buck, J. R., Buell, W. F., Dickinson, R. P., Kozlowski, D. A., Marechal, N. J., and Wright, T. J., "Synthetic-aperture imaging laser radar: laboratory demonstrations and signal processing," Appl. Opt. 44, 7621-7629 (2005).

[6] Barber, Zeb W., and Dahl, Jason R., "Synthetic aperture ladar imaging demonstrations and information at very low return levels," Appl. Opt., 53 (24), 5531-5537 (2014)

[7] Satyan, N., Vasilyev, A., Rakuljic, G., Leyva, V., and Yariv, A., "Precise control of broadband frequency chirps using optoelectronic feedback," Opt. Express 17 (18), 15991 (2009).

[8] Roos, P. A., Reibel, R. R., Berg, T., Kaylor, B., Barber, Z., and Babbitt, W. R., "Ultra-broadband optical chirp linearization for precision length metrology applications," Opt. Lett., 34 (23), 3692-3694 (2009)

[9] Ahn, T-J., Lee, J. Y. and Kim, D. Y., "Suppression of nonlinear frequency sweep in an optical frequency-domain reflectometer by use of Hilbert transformation," Appl. Opt. 44, 7630-7634 (2005).

[10] Nor Azlinah Binti Md Lazam, Koichi Iiyama, Takeo Maruyama, Yosuke Kimura and Nguyen Van T. "Linearization of nonlinear beat frequency in FMCW Interferometer Waveform Modifying Technique," ARPN Journal of Enginerin and Applied Science, 10 (8), 3817-3822 (2015)

[11] Vorontsov, A. M., Vorontsov, M. A., and Gudimetla, V.S. R., "Large-Scale Turbulence Effects Simulations for Piston Phase Retrieval," Proceedings of the 2012 Advanced Maui Optical and Space Surveillance Technologies Conference, (2012).